Assessing Current Parameterization of Mixed-Phase Clouds using In Situ Profiles Measured During the Mixed Phase Cloud Experiment

G.M. McFarquhar and G. Zhang
University of Illinois
Urbana, Illinois

J. Verlinde
Pennsylvania State University
University Park, Pennsylvania

M. Poellot
University of North Dakota
Grand Forks, North Dakota

A. Heymsfield
National Center for Atmospheric Research
Boulder, Colorado

G. Kok
Droplet Measurement Technologies
Boulder Colorado

Introduction

General circulation models (GCMs) suggest that high latitude regions exhibit an enhanced greenhouse warming compared to low latitudes. Data collected during Mixed-Phase Cloud Experiment (MPACE) are critically needed to understand the complex interactions between clouds, the atmosphere and the ocean in the Arctic that can be used to understand feedbacks acting there. Here, we examine vertical profiles of mixed-phase cloud properties obtained during MPACE. These profiles will ultimately be used to determine impacts of clouds on radiation, to evaluate retrievals from remote sensors and to evaluate parameterizations used in large-scale models.

Mixed-Phase Cloud Experiment Microphysics Data

The University of North Dakota (UND) Citation made 11 flights through low-level stratus during MPACE, most of which were mixed-phase. Figure 1 shows a typical flight track from October 5, 2004, with spirals conducted over remote sensing sites at Oliktok Point and Barrow, and porpoising maneuvers flown through cloud in between. Throughout the entire project, 20 spirals were performed over Barrow,

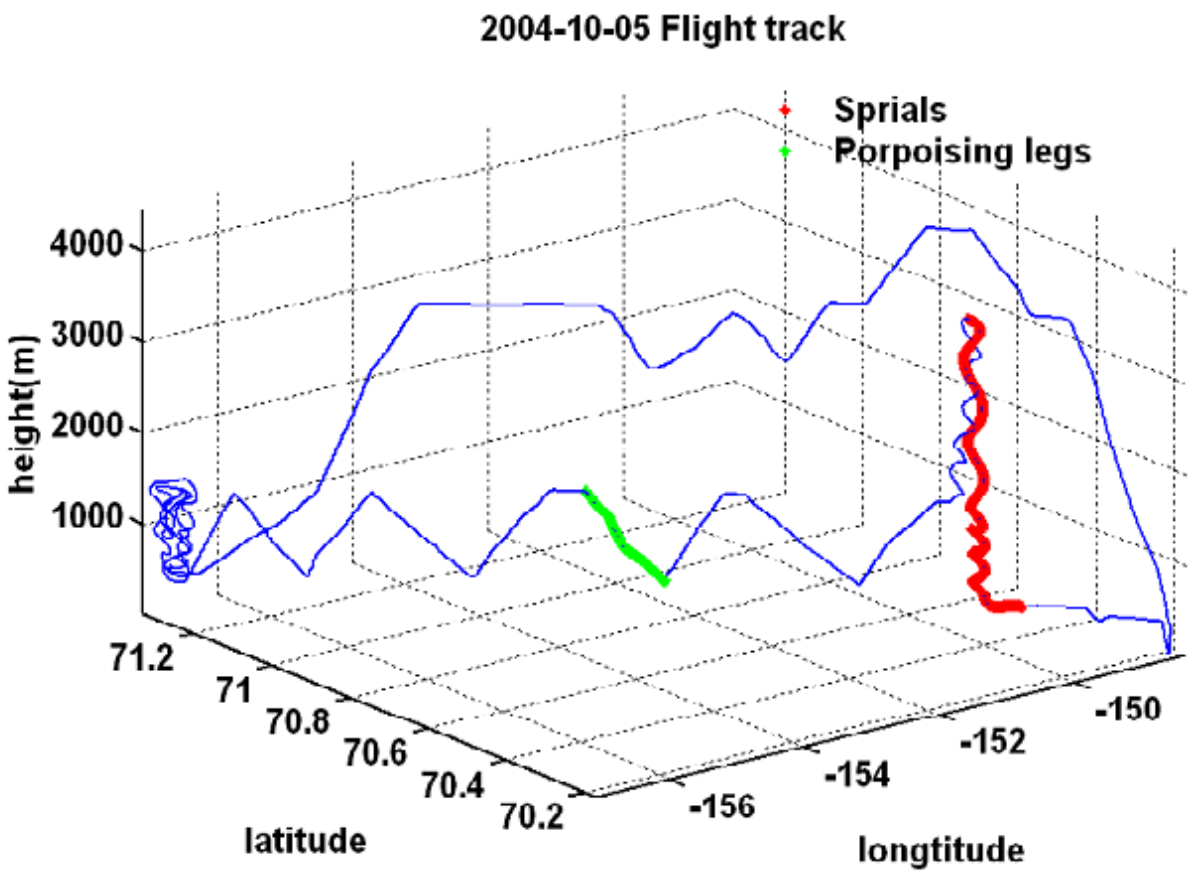

Figure 1. Example of flight tracks from October 5 2004. Spirals over Oliktok Point and Barrow were either Eulerian (fixed in space) or Lagrangian (advect with wind). Between Oliktok Point and Barrow, UND Citation would porpoise through cloud, ideally between the top and bottom of the cloud.

24 over Oliktok Point and 65 porpoising profiles in between, representing 109 vertical profiles. Of these, 71 were complete profiles between tops and bottoms, whereas either base or top was not reached for the other spirals. Table 1 shows the times, locations, cloud top and base altitudes, cloud top and base temperatures, the cloud phase and cloud type (single layer or multi-layer cloud) for all the spirals executed on October 5. Table 1 also notes whether the spirals were Lagrangian (advected with the wind) or Eulerian (fixed in space). Similar tables have been constructed for all other days.

Table 1. Summary of spiral/porpoise legs on Oct. 5 2004, similar tables for all flights document the 16 spirals at Barrow, 21 at Oliktok Point and 64 porpoising legs. Cloud type can be either ice, liquid, or mixed. Clouds consist of multi-cloud layers or single cloud layers.

Start time	End time	Min height (m)	Max height (m)	Max Temp (c)	Min Temp (c)	Track Type	Cloud Type	Cloud layer	Location of spirals
19:23:00	19:29:49	461.7	1420.3	-2.82	-6.55	Lagrangian	Mixed	Multi	Barrow
19:29:50	19:39:49	523.3	1447.2	-3.45	-6.16	Lagrangian	Mixed	Multi	Barrow
19:39:50	19:49:49	450.9	1422.3	-2.84	-6.36	Euler	Mixed	Multi	Barrow
19:49:50	20:04:49	456.1	1430.2	-2.68	-6.64	Euler	Mixed	Multi	Barrow
20:04:50	20:10:09	461.1	1402.6	-2.67	-6.17	Porpoising leg	Mixed	Single	Leg
20:10:10	20:15:49	535.1	1353.5	-3.48	-6.13	Porpoising leg	Mixed	Single	Leg
20.15:50	20:21:29	465.3	1356.6	-2.95	-6.00	Porpoising leg	Mixed	Multi	Leg
20:21:30	20:30:09	460.2	1407.6	-3.01	-6.16	Porpoising leg	Mixed	Multi	Leg
20:30:10	20:38:49	452.4	1435.2	-2.12	-5.20	Porpoising leg	Mixed	Multi	Leg
20:38:50	20:45:09	449.2	1429.7	-3.02	-5.67	Porpoising leg	Mixed	Multi	Leg
20:45:10	20:51:29	455.5	1420.4	-2.97	-5.79	Porpoising leg	Mixed	Multi	Leg
20:51:30	20:59:49	489.2	1414.5	-2.67	-5.91	Porpoising leg	Mixed	Multi	Leg
20:59:50	21:08:09	445.7	1517.7	-2.97	-6.15	Porpoising leg	Mixed	Multi	Leg
21:08:10	21:18:09	1520.3	3487.2	-3.75	-14.24	Lagrangian	Mixed	Multi	Oliktok Point
21:18:10	21:34:49	542.5	3486.6	-3.66	-14.39	Lagrangian	Mixed	Multi	Oliktok Point

The instrumentation on board the Citation is summarized in Table 2. The Citation was equipped with a two-dimensional cloud (2DC) probe effectively measuring size distributions between 125 and 1600 μm, a one dimensional cloud (1DC) probe effectively measuring distributions between 50 and 620 μm, a forward scattering spectrometer probe (forward scattering spectrometer probe [FSSP], measuring between 3.0 and 54.5 μm) and a high-volume precipitation sampler (HVPS, measuring between 400 μm to 4 cm). A CPI provided 2.3 μm resolution images between 15 and 2000 μm. Bulk liquid water content was measured with a King liquid water content (LWC) probe and a Cloud Spectrometer and Impactor (CSI) probe (a newer version of the counterflow virtual impactor (CVI) gave bulk measurements of total water content (TWC). A Rosemount icing detector identified the presence of supercooled water. This combination of probes gives us all the information needed to determine the phase of any cloud sampled and size distributions covering the complete range of possible particle sizes.

Table 2. Microphysical instruments deployed during MPACE

Instruments	Derived Parameters	Nominal Range	Comments
Forward Scattering Spectrometer Probe (FSSP)	PSDs, Nt, LWC	1-55μm	Uncertain in mixed-phase cloud
One-dimensional Cloud Probe (1DC)	PSDs, Nt, LWC	20-620μm	Use between 20-120 μm
Cloud Particle Imager (CPI)	Images (2.3 μm resolution); habit distribution	15-2000μm	Small sample volume
Two-dimensional Cloud Probe (2DC)	PSDs, Nt, LWC/IWC, images	32-960μm	125<D<960μm
High Volume Precipitation Sampler (HVPS)	PSDs, Nt, LWC/IWC, images	400-40000μm	D>960 μm
DMI CSI probe	Total Water Content	Bulk measurement	
King probe	LWC	Bulk measurement	
Rosemount Icing probe	Supercooled Water	Detects presence from voltage change	

Assessment of Bulk Water Measurements

The phase (liquid, ice, or mixed) of each 30-s average size distribution was identified following Cober et al. (2001) and McFarquhar and Cober (2004). Periods with supercooled water were first identified using the Rosemount icing detector. Inspection of CPI, 2DC and HVPS images identified periods with non-spherical particles and hence the presence of ice. Examination of the FSSP size distributions helped determine whether significant amounts of ice was present because FSSP size distributions typically exhibit sharp peaks between 10 and 20 μm when supercooled droplets dominate the total water content, but exhibit a flat signal appears when ice dominates the total water content. A combination of information from these techniques helped unambiguously identify the phase for each 30-second time period. A comparison of the CSI total water content against the King liquid water content typically confirmed the phase identification; in the presence of ice the CSI TWC exceeds the King LWC because the King probe responds mainly to water, whereas the CSI responds to ice and liquid.

After identifying the phase of each 30-second time period, size distributions were derived from the 2DC, HVPS, FSSP and 1DC data. For pure water cases, the FSSP (3-50 μm), 1DC (50-150 μm), 2DC (150-1000 μm) and HVPS (> 1000 μm) concentrations are simply combined to cover the entire size range. Figure 2 shows that good agreement between LWCs estimated from FSSP and 1DC size distributions against the bulk LWCs measured by the King and CSI probes for liquid conditions is obtained, suggesting measurements from different probes are consistent for liquid conditions. FSSP data cannot typically be used quantitatively for glaciated conditions as Gardiner and Hallett (1985) and Cober et al (2001) showed that FSSP channels larger than 30 μm were biased by responses to ice when ice concentrations for 2DC crystals larger than 125 μm exceeded 1 L-1; the resulting flat FSSP signal was not a true SD. McFarquhar and Cober (2004) also suggested that FSSP data could describe size distributions of supercooled drops for mixed-phase clouds whenever 2DC concentrations were smaller than 1 L-1; preliminary indications are that such conclusions also apply to MPACE data as seen from the analysis of the size distributions and bulk total water contents described below.

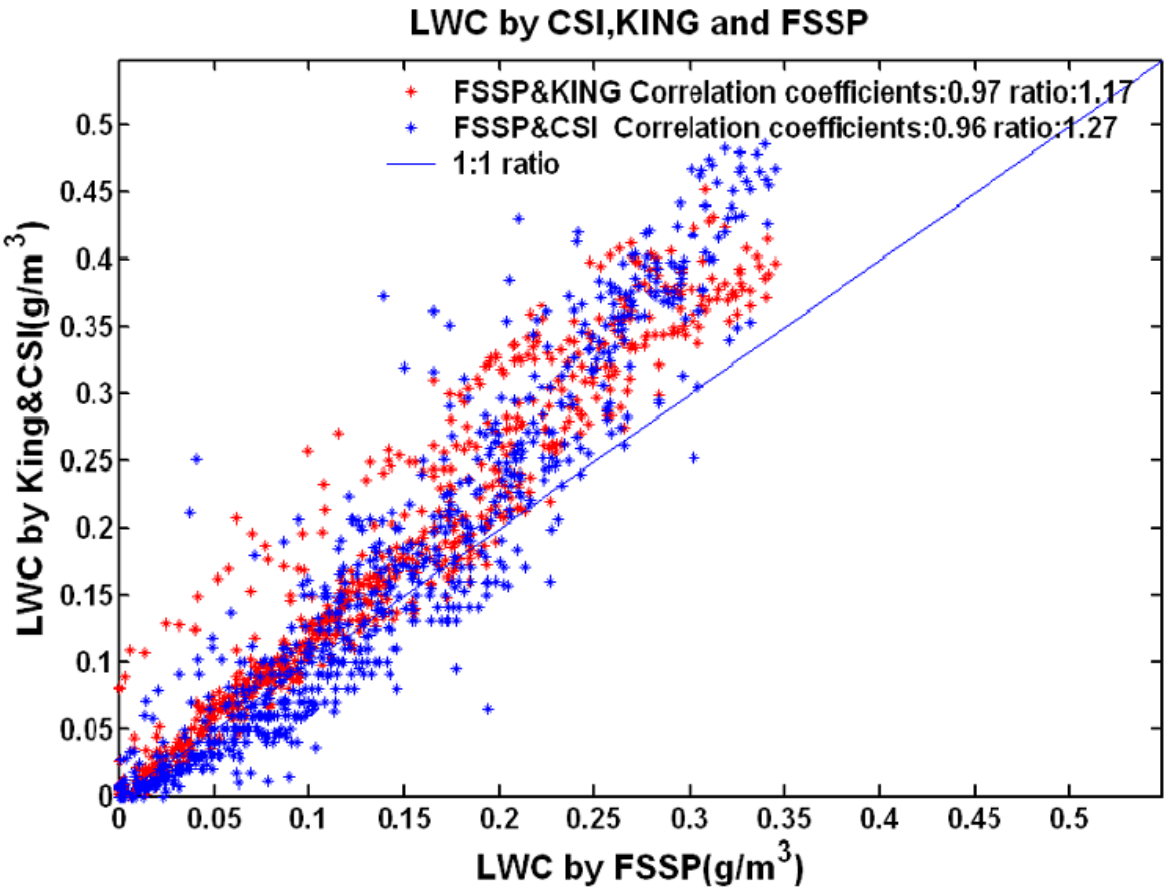

Figure 2. Bulk LWC from King/CSI vs. LWC derived from FSSP PSD. For LWC < 0.2 g m^{-3}, King and CSI measurements differ from FSSP by 9% and 21% respectively; for LWC > 0.2 g m^{-3}, King and CSI measurements differ from FSSP by 25% and 29% respectively. Data are shown for time periods with no ice particles seen in 2DC and CPI images and 2DC concentrations < 0.1 L-1.

Size-Resolved Properties

On October 10, 2004, an approximately 400 m thick cloud was observed by the Pacific Northwest National Laboratory (PNNL) Atmospheric Remote Sensing Laboratory (PARSL) lidar over Oliktok Point. This cloud, located under a sharp inversion, persisted through most of the MPACE domain; 9 spirals over Barrow and Oliktok Point together with 20 porpoises were executed to characterize its vertical variability. It is an obvious choice for an initial examination of the structure of mixed-phase clouds because it occurred in a single layer and does not have the complication of multiple layers that were observed on other days. Figures 3 and 4 show size distributions measured over Oliktok Point within this single-layer mixed-phase cloud at a time when the lidar detected cloud base was at 900 m and a strong liquid layer occurred near cloud top at 1300 m. At this time, the cloud radar also indicated the occurrence of patches of large ice crystals in the liquid cloud layer and precipitating ice crystals beneath. Good overlap between probes in Figure 3 suggests that the probes were behaving reasonably. Liquid layers are seen by strong peaks in the FSSP size distributions around 20 μm, with the modal

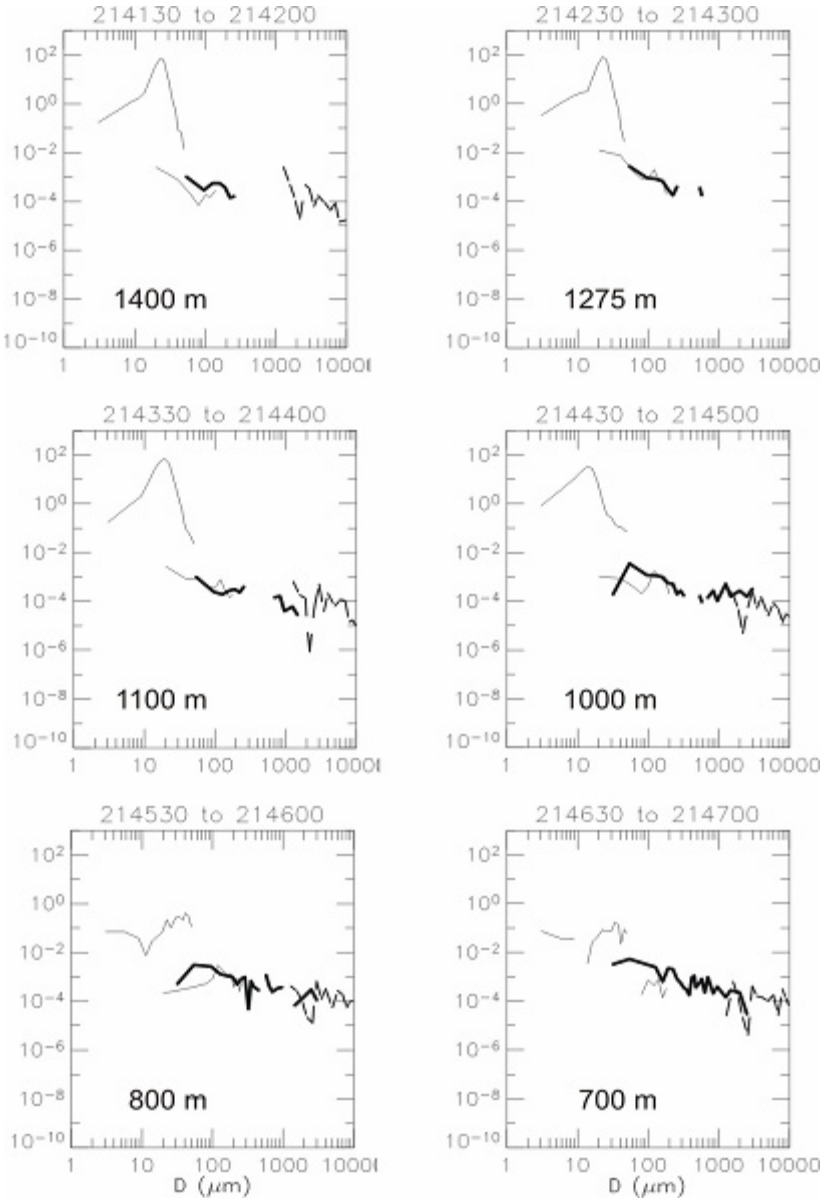

Figure 3. Example 30-s averaged size distributions measured October 10, 2004 in vertical profile flown by UND Citation between 2140 and 2147 GMT.

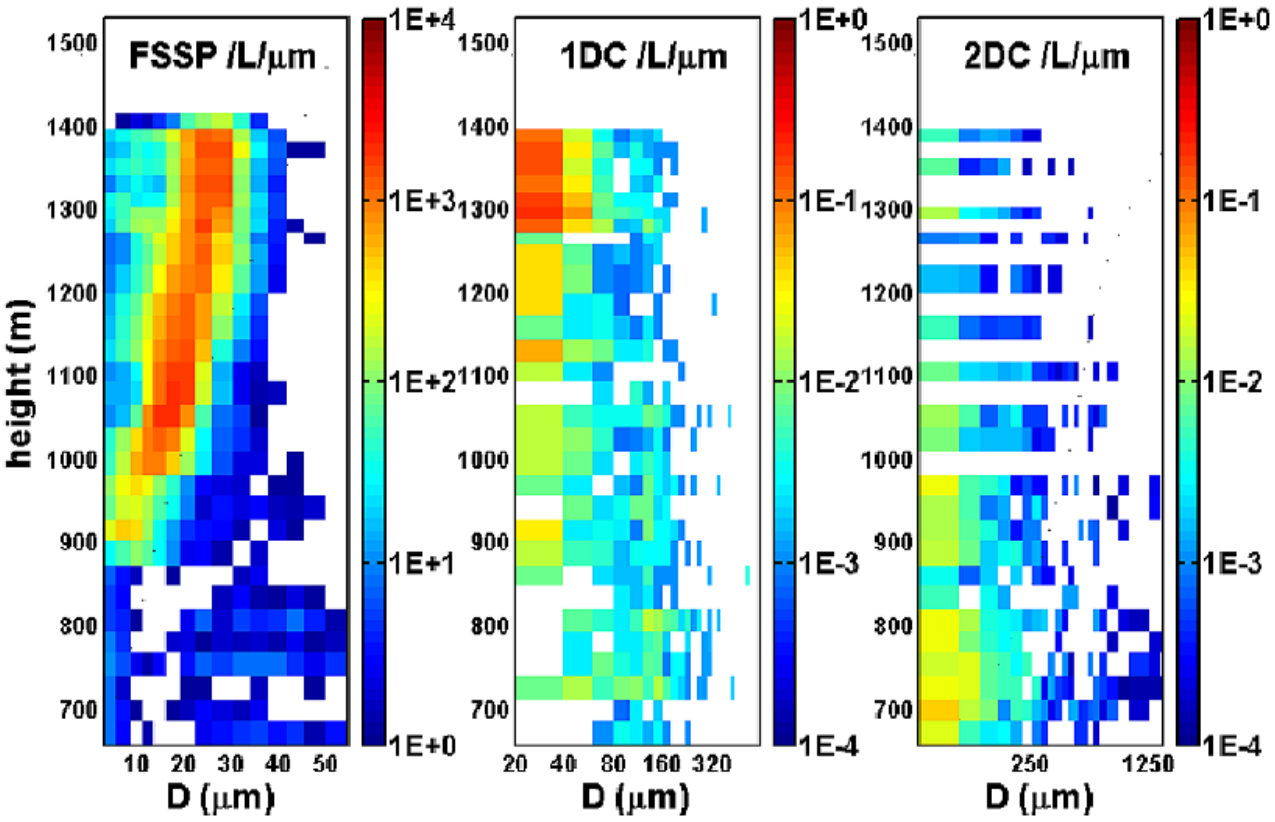

Figure 4. Vertical profile of 10-s averaged size distributions for same case as in Figure 3.

diameter increasing with height, eventually producing drizzle drops with sizes above 20 μm. In general, greater numbers of large crystals, corresponding to ice, are seen near cloud base (1000 and 1100 m) and precipitating beneath cloud (700 and 800 m), but ice occurs in patches throughout and even at the top of the cloud. These conclusions are reaffirmed by inspection of Figure 5 showing the CPI, 2DC and HVPS images for a spiral ascent over Oliktok Point. Drizzle is seen near cloud top (1200-1500 m) from the circular CPI images, but the larger 2DC and HVPS images, with irregular and rimed shapes, indicate ice. Note that even though large ice crystals are more frequent near and below cloud base, they occur throughout cloud.

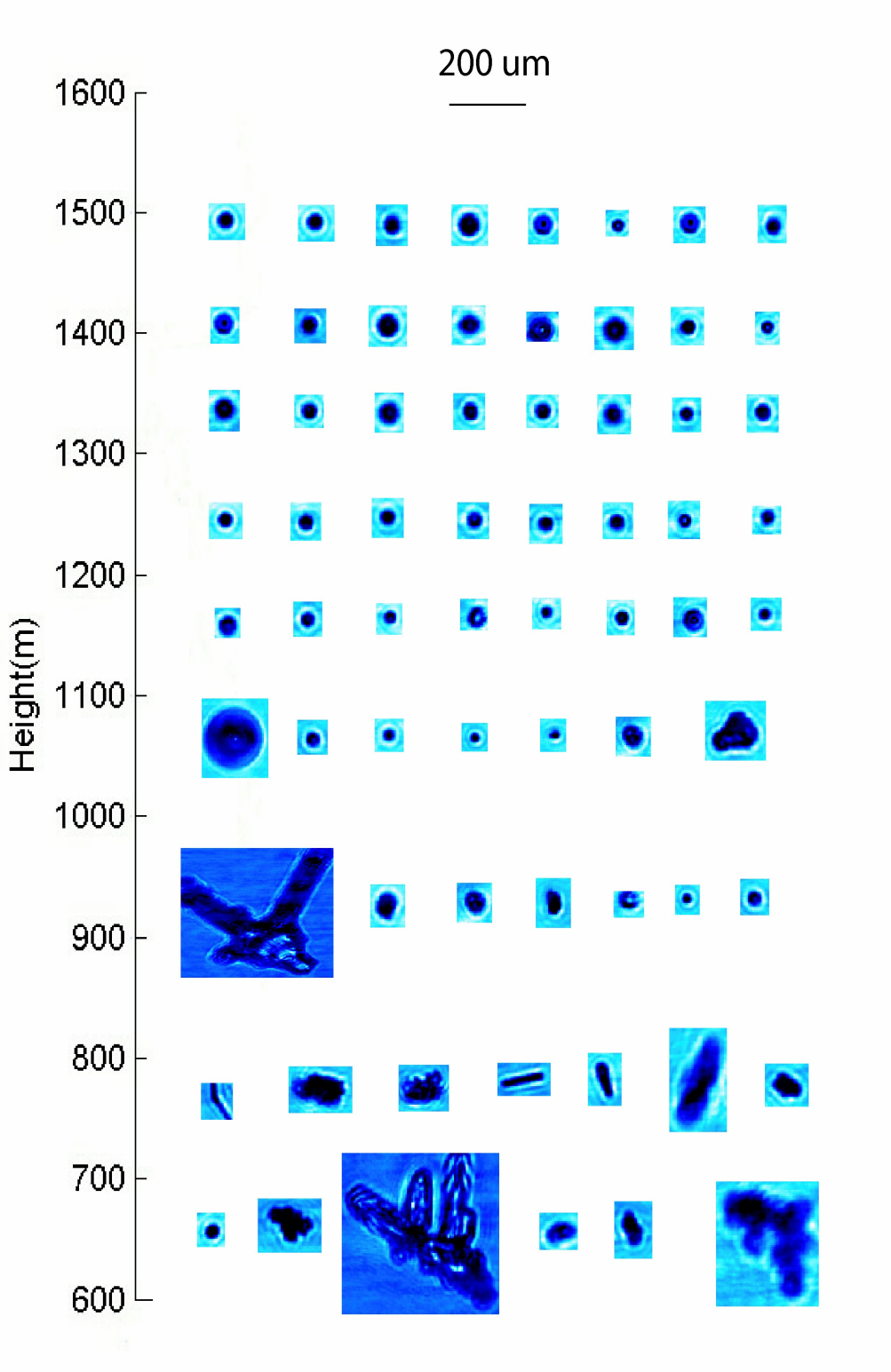
200 um
Height(m)
1600
1500
1400
1300
1200
1100
1000
900
800
700
600

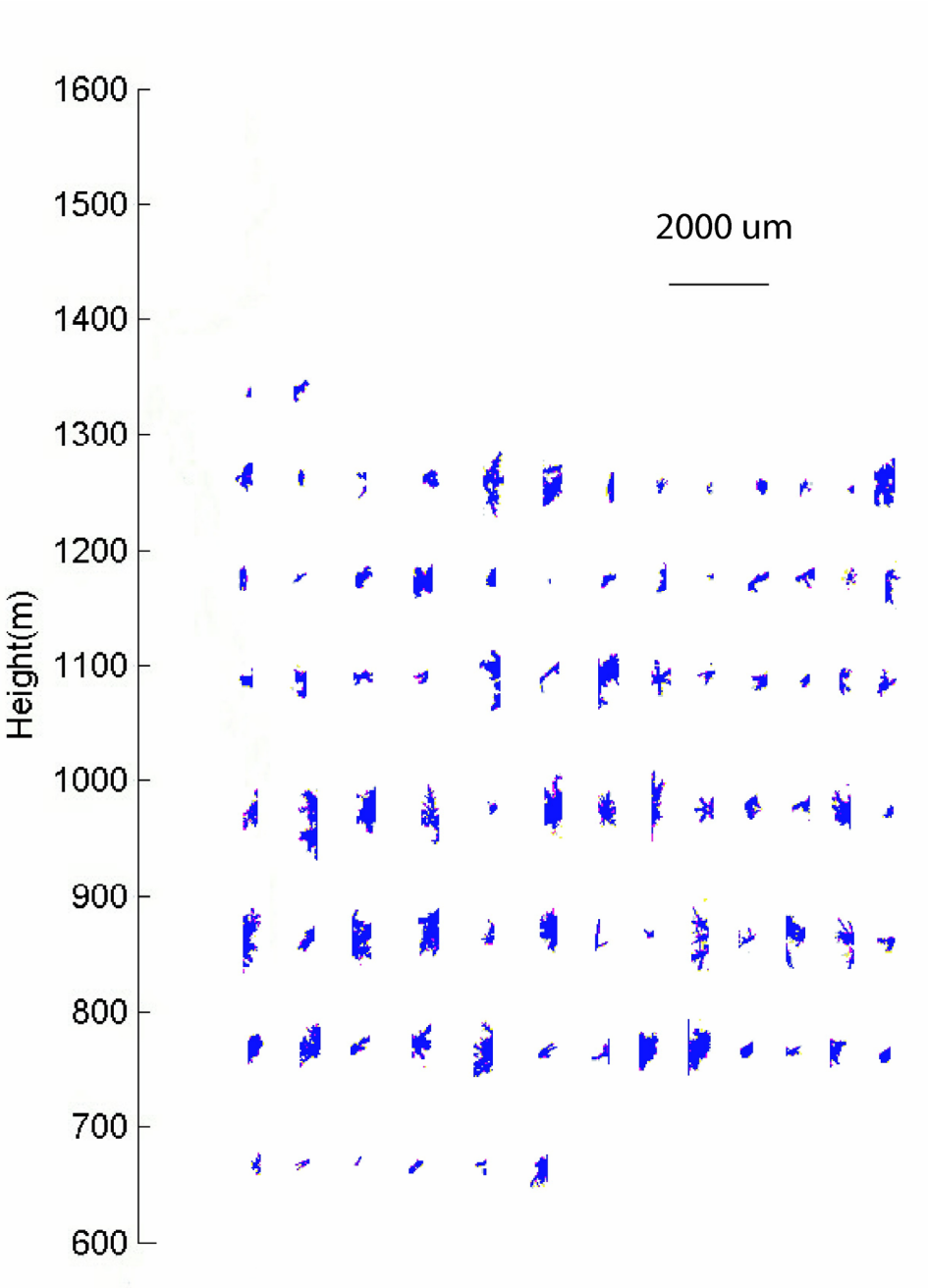

Figure 5. Example of selected CPI (left), 2DC (middle) and HVPS (right) images acquired for vertical profile shown in Figure 3 and Figure 4. Smaller spherical images near cloud top (CPI) are small drizzle or supercooled drops. Larger ice crystal images show dominance of irregular and rimed crystal shapes. Even though the largest crystals measured by HVPS are more frequent near and below cloud base, they can occur throughout depth of cloud.

Bulk Properties

The size distributions calculated in Section 4 are used to determine how the bulk properties of the size distributions vary with altitude and temperature. The mass of supercooled water drops is obtained by integrating FSSP distributions (and 1DC distributions if drizzle is present in CPI images) with respect to size. To derive ice water content (IWC) from the ice crystal size distributions measured by the 2DC and HVPS, published relationships between mass and maximum dimension (e.g., Locatelli and Hobbs 1974; Brown and Francis 1995; Mitchell 1996) and between mass, maximum dimension and area ratio (Heymsfield et al. 2002) for different habits are used. The choice of scheme has a significant impact on IWC. Figure 6 shows bulk IWC, derived by subtracting the FSSP/King LWC from the CSI TWC, against IWC estimated by applying different mass calculation techniques to the measured 1DC/2DC/HVPS size distributions. Reasonable agreement is noted suggesting the MPACE measurements are internally consistent, but large differences between schemes is seen. We are currently further assessing the best mass-diameter relationships to describe the ice crystals imaged during MPACE.

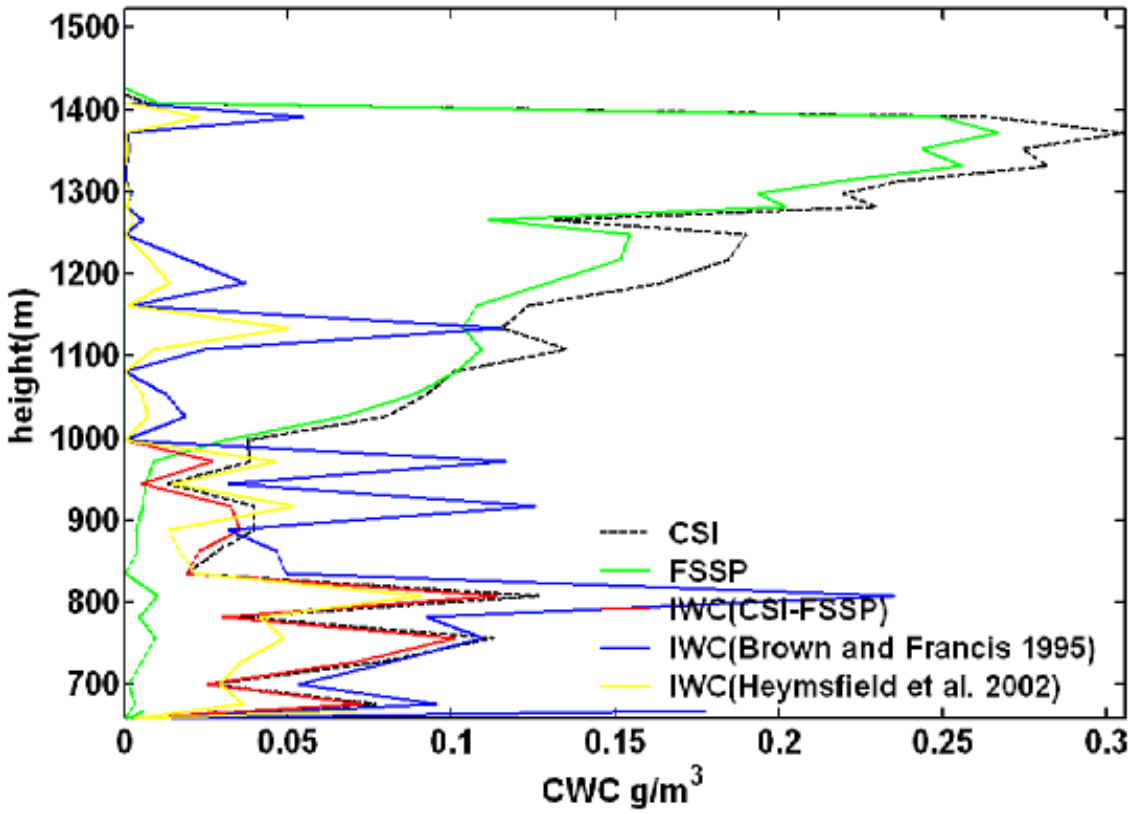

Figure 6. Comparison of bulk measurements of IWC (CSI-FSSP) against IWC estimated from 2DC using variety of habit identification and mass calculation techniques.

Cloud top altitude gradually increased from 1300 m to 1400 m during the time over which the spirals were conducted over Oliktok Point on October 10 (Verlinde et al. 2005). Hence, in order to visualize data from several spirals simultaneously, vertical profiles made on October 10 are plotted together as a function of normalized cloud altitude Zn where Zn varies from 1.0 at cloud top to 0.0 at cloud base. Each blue dot in Figure 7 through Figure 9 represents the quantity measured at the given normalized height for a single spiral on October 10 and the red line represents the average of that quantity all spirals. A clear trend of increasing liquid fraction with increasing height is seen with the cloud being almost entirely liquid at cloud top. This suggests that parameterizations for effective cloud fraction in large-scale models that are functions of only temperature may not adequately represent the behavior of mixed-phase clouds where the liquid fraction is highly sensitive to the position within the cloud. The water droplet effective radius increases with height due to condensational growth and the eventual production of drizzle by collision-coalescence near cloud top. However, the ice crystal effective radius defined following Fu (1996) shows little systematic change with altitude. Similar plots are being constructed for all other days that were sampled during MPACE.

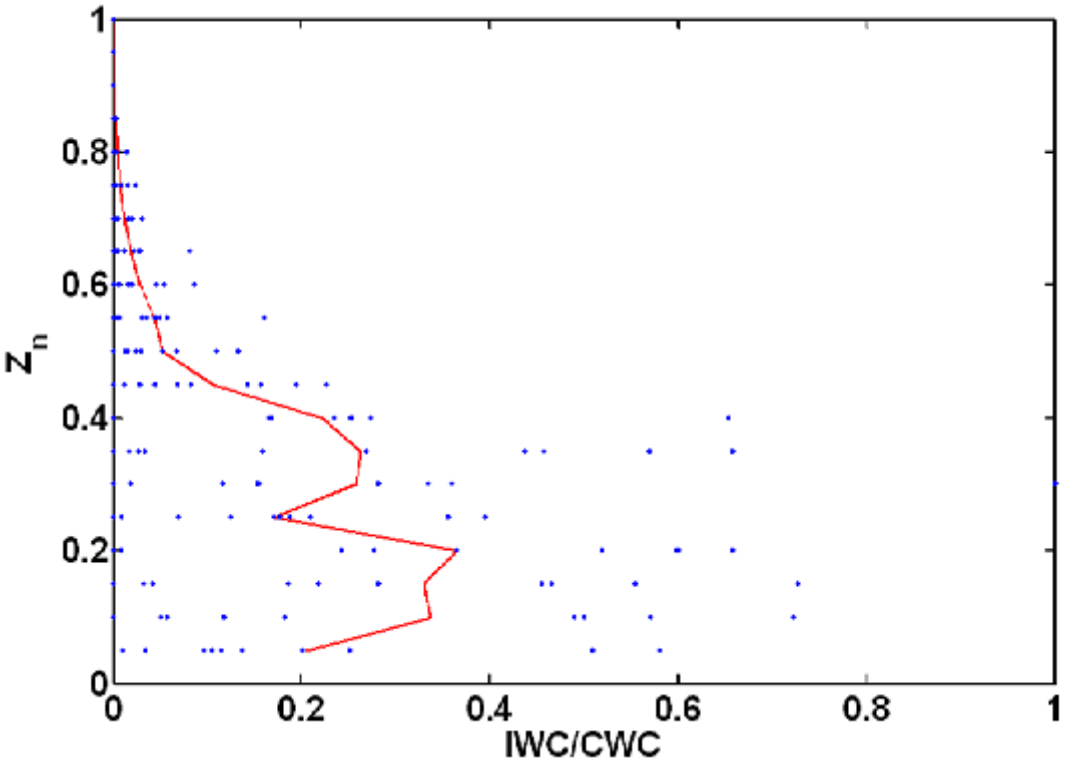

Figure 7. Vertical variation of fraction of IWC/CWC in terms of normalized height. Dominance of water near cloud top and ice near cloud base (for some cases) is seen.

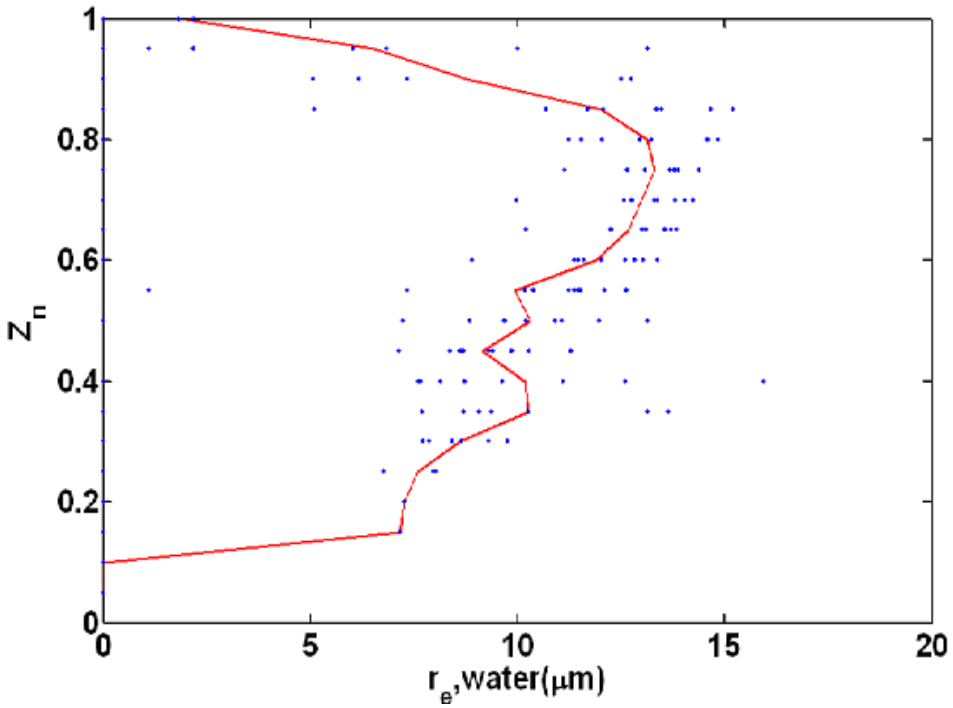

Figure 8. As in Figure 7, except for vertical variation of water droplet effective radius.

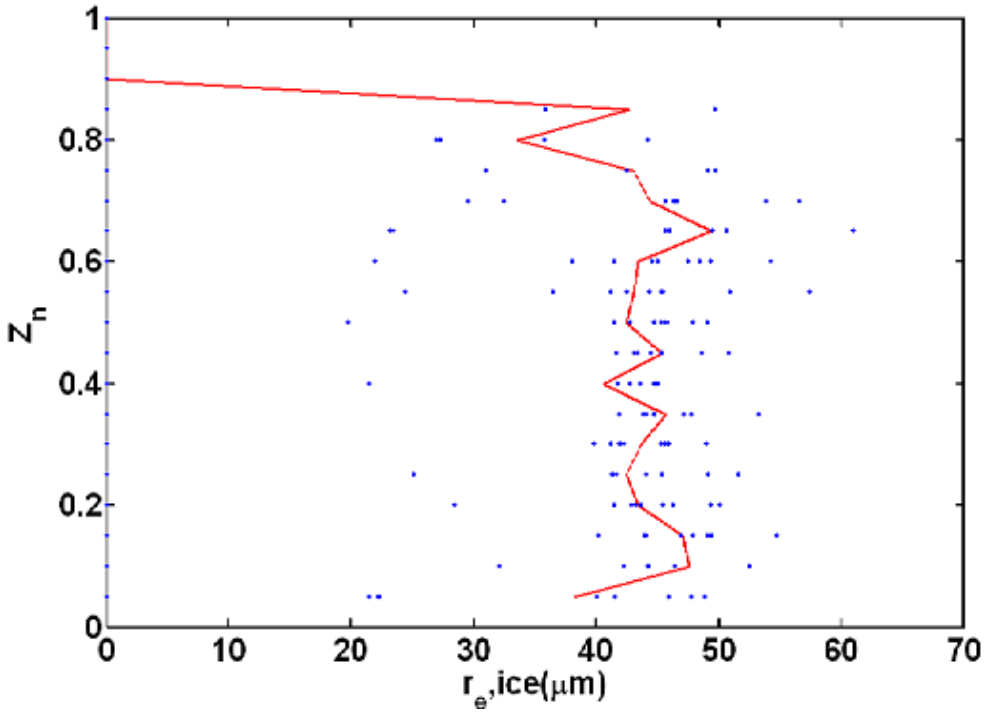

Figure 9. As in Figure 8, except for ice crystal effective radius.

Summary

An initial examination of the microphysical data collected in mixed-phase clouds during MPACE has shown that the probes performed well and that much data were obtained to characterize the vertical profiles of mixed-phase clouds. Examination of data collected in single-layer clouds has shown clear trends in how microphysical parameters vary with normalized cloud altitude that may differ from parameterizations of mixed-phase clouds used in large-scale models, where quantities mainly depend on the temperature of clouds.

In addition to the single-layer cases analyzed here, there are also examples of multi-layer mixed-phase clouds observed during MPACE. Figure 10 shows an example of the more complex patterns from these multi-layer clouds. Efforts are currently underway to generalize these cases as well. We are also attempting to explore the implications of our findings on the vertical structure of mixed-phase clouds for determinations of radiative fluxes throughout cloud and for cloud radiative heating rates.

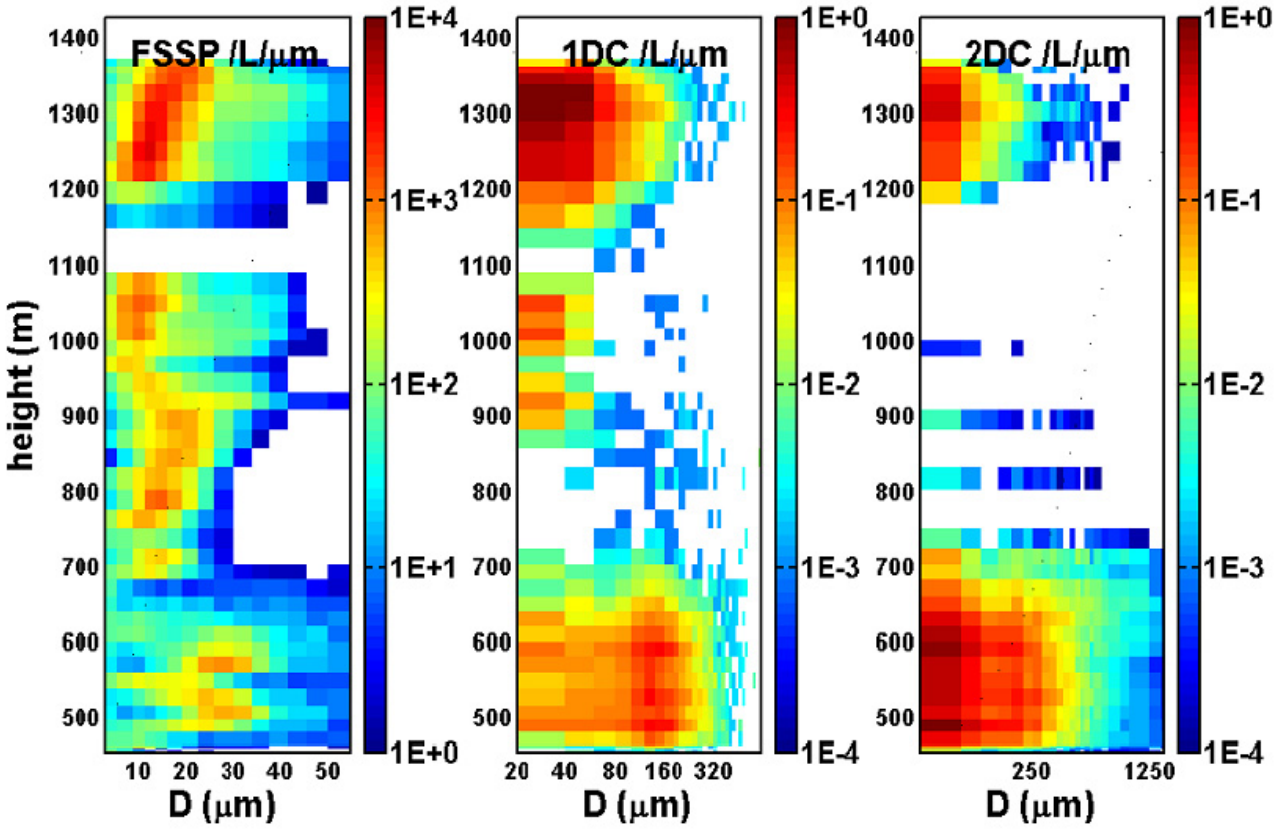

Figure 10. Vertical profile of 10-s averaged size distributions for a multi-layer case.

Acknowledgments

This research was supported by DOE ARM under contract number DE-FG03-00ER62913, Wanda Ferrell program manager. Data were obtained from the ARM archive sponsored by the U.S. Department of Energy, Office of Science, Office of Biological and Environmental Research, Environmental Sciences Division.

References

Brown, PRA, and PN Francis. 1995. "Improved measurement of the ice water content in cirrus using a total water evaporator." *Journal of Atmospheric and Oceanic Technology* 12:410-414.

Cober, SG, GA Isaac, AV Korolev, and JW Strapp. 2001. "Assessing cloud-phase conditions." *Journal of Applied Meteorology* 40:1967-1983

Fu, Q. 1996. "An accurate parameterization of the solar radiative properties of cirrus clouds for climate models." *Journal of Climate* 9:2058-2082.

Gardiner, BA, and J Hallett. 1985. "Degradation of in-cloud forward scattering spectrometer probe measurements in the presence of ice particles." *Journal of Atmospheric and Oceanic Technology* 2:171-180.

Locatelli, JD, and PV Hobbs. 1974. "Fall speeds and masses of solid precipitation particles." *Journal of Geophysical Research* 79:2185-2197.

Heymsfield, AJ, S Lewis, A Bansemer, J Iaquinta, LM Miloshevich, M Kajikawa, C Twohy, and MR Poellot. 2002. "A general approach for deriving the properties of cirrus and stratiform ice cloud particles." *Journal of Atmospheric Science* 59(1), 3-29.

McFarquhar, GM, and SG Cober. 2004. "Single-Scattering Properties of Mixed-phase Arctic Clouds at Solar Wavelengths: Impacts on Radiative Transfer." *Journal of Climate* 17:3799–3813.

Mitchell, DL. 1996. "Use of mass- and area- dimensional power laws for determining precipitation particle terminal velocities." *Journal of Atmospheric Science* 53:1710-1723.

Verlinde, J, YA Harrington, GM McFarquhar, JH Mather, D Turner, B Zak, MR Poellot, T Tooman, AJ Prenni, G Kok,E Eloranta, A Fridlind, C Bahrmann, K Sassen, PJ DeMott, and AJ Heymsfield.. 2005. "Overview of the Mixed-Phase Arctic Cloud Experiment (M-PACE). Eighth Conference on Polar Meteorology and Oceanography, San Diego, CA, American Meteorological Society.